THE STRUCTURE AND PHOTOCHROMISM OF 2,4,4,6-TETRAPHENYL-4*H*-THIOPYRAN

Jaroslav VOJTĚCHOVSKÝ, Jindřich HAŠEK, Stanislav NEŠPŮREK
and Mojmír ADAMEC

Institute of Macromolecular Chemistry, Czechoslovak Academy of Sciences, 162 06 Prague 6

Received September 25, 1991
Accepted November 5, 1991

2,4,4,6-Tetraphenyl-4*H*-thiopyran, $C_{29}H_{22}S$, orthorhombic, $Pna2_1$, a = 17·980(4), b = 6·956(2), c = 34·562(11) Å, V = 4 323(2) Å^3, Z = 8, D_x = 1·237 g cm^{-3}, D_o = 1·23(1) g cm^{-3}, $F(000)$ = = 1 696, $\lambda(\mathrm{CuK}_\alpha)$ = 1·54184 Å, μ = 1·372 mm^{-2}, T = 294 K. The final R was 0·050 for the unique set of 3 103 observed reflections. The central 4*H*-thiopyran ring forms a boat conformation for both symmetrically independent molecules with average boat angles 4·4(3) and 6·8(3)° at S and C(sp^3), respectively. The mean planes of phenyls at the positions 2 and 6 are turned from the double plane of 4*H*-thiopyran by 42·5(5) and 35·8(3)°, respectively. The investigated material undergoes a photochromic change in the solid state after irradiation with UV light or X-rays. The maximum of the new absorption band is situated at 564 nm. The non-exponential time dependence of photochromic bleaching is analysed in terms of a dispersive first-order reaction.

Reversible photochemical recording systems, which are expected to replace magnetic recording devices, continue to attract much interest. A good quality recording system is expected to be based on fully reversible and sufficiently fast photochromic compounds. The photochromic phenomenon may be schematically written as a photoreversible reaction between Y and Z

$$\mathrm{Y}(\lambda_1) \underset{h\nu_2}{\overset{h\nu_1}{\rightleftarrows}} \mathrm{Z}(\lambda_2)$$

with absorption at the wavelength λ_1 and λ_2, respectively. In general, $h\nu_1$, which is radiation that causes the photochromic reaction, is associated with electromagnetic energies lying mostly in the ultraviolet region. This is the activating radiation which enables a conversion of the Y system to the Z system; the latter is thermodynamically less stable and spontaneously reverts to Y. In many cases, the reversion to Y may be accelerated by $h\nu_2$, radiation which generally resides in the visible or infrared region of the spectrum.

Many photochromic materials and mechanisms have been discussed in detail in several review articles and monographs[1-3]. At present, photochromic materials may be considered to be in the stage of development. Wide applications stimulate synthesis of new stable photochromic systems and a study of their photochemical behaviour. It has been known for a long time[4,5] that 2,4,4,6-tetraphenyl-1,4-dihydropyridine and some of its derivatives[6,7] turn red or blue when irradiated with UV or sunlight.

The photochromic behaviour of various 2,4,4,6-tetraphenyl-4*H*-pyrans, 2,4,4,6-tetraphenyl-1,4-dihydropyridines and 1,2,4,4,6-pentaphenyl-1,4-dihydropyridines was reported later[8,9].

It could be mentioned that some thio analogues also show photochromism[10]. In this paper the crystal structure of 2,4,4,6-tetraphenyl-4*H*-thiopyran (*I*) and preliminary photochromic properties are reported. The crystal and molecular structure has been solved using X-ray structure analysis. The structure and properties are compared with those of 2,4,4,6-tetraphenyl-4*H*-pyran[11] (*II*) and 2,4,4,6-tetraphenyl-1,4-dihydropyridine[12] (*III*).

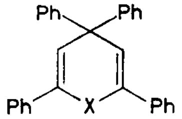

I, X = S
II, X = O
III, X = NH

EXPERIMENTAL

Crystals of the title compound, the synthesis of which has been described elsewhere[10], were freely crystallized from heptane–benzene solution. The measured sample was a prism with dimensions 0·7 × 0·5 × 0·4 mm and turned violet during the X-ray measurement. The space group and cell dimensions were determined from 15 reflections with $19{\cdot}5 < 2\Theta < 30{\cdot}5°$. A total of 3 368 unique reflections were collected on SYNTEX P2$_1$ using the $\Theta - 2\Theta$ technique, of which 3 103 were taken as observed [$I > 0{\cdot}96\sigma(I)$]. The intensities were measured up to $2\Theta = 120°$ with $h = 0/20$, $k = 0/7$, $l = -38/0$. Three standard reflections (410, $\bar{2}0\bar{2}$, 004) showed no significant fluctuations during the measurement and colouration of the crystal.

The phase problem was solved by direct methods using[13] MULTAN 87. The structure was refined in two blocks by the full-matrix least square technique using[14] SHELX 76. Scattering factors were taken from tables[15]. All atomic coordinates, the anisotropic temperature factors for non-H atoms and the isotropic temperature factors for hydrogens were refined till shifts of all 721 parameters fell below 0·19 of their e.s.d.'s. The z coordinate of S1A was fixed during the refinement because of a definition of an origin in the $Pna2_1$ space group. The function minimized was $\sum(w(|F_o| - |F_c|)^2)$, where $w = (\sigma^2(F_o) + 0{\cdot}0009|F_o|^2)^{-1}$. In the final stage an isotropic extinction factor was refined to $0{\cdot}437 \, . \, 10^{-6}$. Final $R = \sum(|F_o| - |F_c|)/\sum|F_o| = 0{\cdot}050$, $R_g = (\sum w(|F_o| - |F_c|)^2/\sum w|F_o|^2)^{-1/2} = 0{\cdot}066$. The geometry was calculated with a program[16] PARST.

The optical spectra and kinetics of photochromism of crystalline powder were determined from measurements of diffuse reflection in air by means of a recording spectrophotometer CF-4 Optica Milano.

RESULTS AND DISCUSSION

There are two symmetrically independent molecules of *I* in the unit cell, denoted A and B, respectively. The numbering scheme and thermal ellipsoids with the 50% probability level for *I* are drawn in Fig. 1. The fractional coordinates and equivalent isotropic thermal parameters are listed in Table I, the coordinates of hydrogens and

TABLE I

Final coordinates (.10^4) and equivalent isotropic thermal parameters U_{eq} (.10^4, Å^2) with estimated standard deviations (e.s.d.'s) in parentheses for the non-H atoms ($U_{eq} = \frac{1}{3}\sum_i \sum_j U_{ij} a_i^* a_j^* \mathbf{a}_i \mathbf{a}_j$)

Atom	x	y	z	U_{eq}	Atom	x	x	z	U_{eq}
S1A	−672(1)	5889(1)	−99(1)	580(9)	S1B	2932(1)	4071(2)	−3697(1)	694(9)
C2A	−9(2)	4450(5)	−338(1)	459(9)	C2B	2262(2)	5490(5)	−3466(1)	486(9)
C3A	221(2)	4716(6)	−702(1)	488(8)	C3B	2023(2)	5228(6)	−3106(1)	543(9)
C4A	−32(2)	6229(5)	−984(1)	471(9)	C4B	2275(2)	3705(6)	−2814(1)	517(8)
C5A	−692(2)	7387(6)	−833(1)	516(9)	C5B	2932(2)	2575(7)	−2967(1)	574(9)
C6A	−972(2)	7382(6)	−480(1)	491(9)	C6B	3220(2)	2588(6)	−3323(1)	535(9)
C21A	304(2)	2925(6)	−87(1)	476(9)	C21B	1964(2)	6994(6)	−3729(1)	495(9)
C22A	499(3)	3283(7)	293(1)	628(9)	C22B	1807(3)	6634(8)	−4118(1)	649(9)
C23A	823(3)	1885(8)	525(1)	739(9)	C23B	1484(3)	8057(9)	−4344(2)	798(8)
C24A	953(3)	58(8)	365(1)	727(9)	C24B	1312(3)	9812(9)	−4203(2)	757(9)
C25A	764(3)	−317(7)	−8(1)	656(8)	C25B	1487(3)	10219(8)	−3817(2)	717(9)
C26A	449(3)	1114(6)	−236(2)	552(9)	C26B	1802(3)	8828(7)	−3587(2)	575(8)
C61A	−1584(2)	8743(6)	−366(1)	512(9)	C61B	3838(2)	1293(6)	−3437(1)	542(9)
C62A	−1580(3)	10602(7)	−506(2)	669(9)	C62B	4411(3)	1840(8)	−3686(1)	667(9)
C63A	−2147(3)	11862(8)	−414(2)	774(9)	C63B	4978(3)	555(9)	−3771(2)	761(9)
C64A	−2709(3)	11311(8)	−163(2)	785(9)	C64B	4983(3)	−1230(8)	−3630(2)	815(8)
C65A	−2708(3)	9457(8)	−10(2)	752(9)	C65B	4428(3)	−1832(8)	−3394(2)	778(9)
C66A	−2149(2)	8206(7)	−114(1)	663(9)	C66B	3841(3)	−602(6)	−3296(1)	660(9)
C411A	605(2)	7685(6)	−1067(1)	504(9)	C411B	1648(2)	2241(6)	−2733(1)	503(8)
C412A	480(3)	9242(6)	−1319(1)	574(9)	C412B	950(3)	2386(7)	−2906(1)	603(8)
C413A	1031(3)	10575(7)	−1387(2)	713(8)	C413B	403(3)	1024(7)	−2836(2)	705(9)
C414A	1706(3)	10431(7)	−1213(2)	757(9)	C414B	539(3)	−482(8)	−2591(2)	737(9)
C415A	1840(3)	8927(8)	−969(2)	704(9)	C415B	1210(4)	−638(7)	−2413(2)	726(9)
C416A	1284(3)	7541(6)	−899(1)	546(9)	C416B	1771(3)	736(6)	−2484(1)	630(8)
C421A	−271(2)	5163(5)	−1358(1)	483(9)	C421B	2512(2)	4798(6)	−2444(1)	515(8)
C422A	−918(3)	4036(7)	−1348(2)	667(9)	C422B	2096(3)	4752(7)	−2104(1)	626(9)
C423A	−1127(3)	2974(8)	−1671(2)	864(9)	C423B	2311(é)	5838(8)	−1786(2)	769(9)
C424A	−706(4)	3005(8)	−2006(2)	808(9)	C424B	2945(3)	6980(8)	−1810(2)	912(9)
C425A	−81(3)	4122(8)	−2018(2)	740(9)	C425B	3351(3)	6999(8)	−2138(2)	863(9)
C426A	129(2)	5200(7)	−1696(1)	577(9)	C426B	3145(3)	5964(7)	−2460(2)	716(9)

TABLE II

Final coordinates (.10^3) and isotropic thermal parameters U_{iso} (.10^3, Å^2) with e.s.d.'s in parentheses for H atoms

Atom	x	y	z	U_{iso}	Atom	x	y	z	U_{iso}
H3A	56(2)	369(5)	−85(1)	41(9)	H3B	154(2)	622(6)	−303(1)	49(11)
H5A	−90(2)	834(6)	−104(1)	42(9)	H5B	334(3)	174(8)	−278(1)	72(14)
H22A	25(3)	446(8)	40(2)	77(15)	H22B	182(2)	556(7)	−423(1)	44(12)
H23A	101(3)	191(7)	77(2)	63(13)	H23B	157(3)	777(7)	−461(2)	70(15)
H24A	114(3)	−119(8)	52(2)	85(17)	H24B	99(3)	1083(7)	−436(1)	69(13)
H25A	76(3)	−169(7)	−16(1)	66(12)	H25B	134(3)	1169(8)	−374(1)	70(14)
H26A	37(2)	91(6)	−43(1)	42(14)	H26B	199(2)	909(5)	−330(1)	35(9)
H62A	−104(3)	1104(8)	−66(2)	94(17)	H62B	435(2)	294(7)	−373(1)	46(12)
H63A	−226(4)	1335(9)	−60(2)	110(19)	H63B	536(4)	102(9)	−390(2)	114(19)
H64A	−213(3)	1259(9)	−9(2)	104(17)	H64B	538(2)	−182(6)	−378(1)	59(12)
H65A	−308(2)	899(6)	18(1)	46(10)	H65B	436(3)	−338(8)	−335(2)	78(14)
H66A	−213(2)	670(6)	7(1)	56(11)	H66B	343(2)	−113(5)	−213(1)	46(10)
H412A	1(3)	925(6)	−142(1)	62(14)	H412B	97(3)	336(9)	−311(2)	86(16)
H413A	96(3)	1164(8)	−159(1)	67(13)	H413B	−13(4)	123(9)	−300(2)	117(19)
H414A	210(2)	1125(7)	−133(1)	56(12)	H414B	20(3)	−136(8)	−257(2)	77(16)
H415A	225(3)	8795(6)	−87(1)	51(12)	H415B	128(3)	−144(9)	−226(2)	69(16)
H416A	142(2)	640(6)	−71(1)	46(10)	H416B	226(3)	74(6)	−233(1)	61(13)
H422A	−125(2)	403(5)	−111(1)	30(8)	H422B	158(3)	405(8)	−214(2)	87(18)
H423A	−158(5)	229(9)	−171(3)	166(29)	H423B	193(4)	596(9)	−150(3)	130(19)
H424A	−89(3)	207(8)	−220(2)	77(15)	H424B	309(4)	768(9)	−152(2)	110(19)
H425A	18(3)	391(7)	−225(2)	63(13)	H425B	370(4)	793(9)	−228(2)	96(19)
H426A	54(2)	599(6)	−170(1)	46(11)	H426B	304(5)	623(9)	−277(3)	165(19)

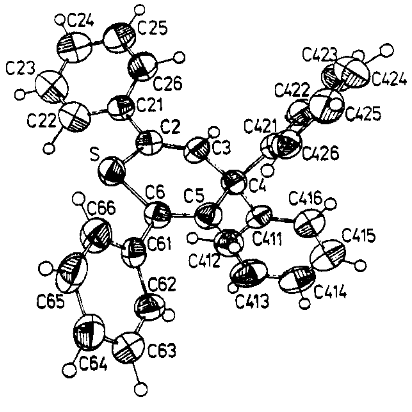

FIG. 1

Numbering scheme of *I* with thermal ellipsoids their isotropic thermal parameters in Table II. Both distances and selected bond angles are listed in Table III.

The crystal structure of *I* has no intermolecular contacts between non-H atoms shorter than 3·4 Å. The stereoscopic view of the unit cell is shown in Fig. 2. We

TABLE III

Bond lengths (Å) and selected bond angles (°) with e.s.d.'s in parentheses

Bond	Bond length		Bond	Bond length	
	A	B		A	B
S1—C2	1·762(3)	1·750(3)	S1—C6	1·762(4)	1·733(4)
C2—C3	1·337(5)	1·329(5)	C2—C21	1·481(3)	1·486(3)
C3—C4	1·505(3)	1·532(3)	C4—C5	1·525(3)	1·514(3)
C4—C411	1·556(2)	1·545(2)	C4—C421	1·551(4)	1·548(4)
C5—C6	1·321(5)	1·335(5)	C6—C61	1·504(2)	1·484(2)
C21—C22	1·382(5)	1·396(5)	C21—C26	1·386(2)	1·398(2)
C22—C23	1·388(3)	1·388(3)	C23—C24	1·405(2)	1·350(2)
C24—C25	1·359(5)	1·400(5)	C25—C26	1·390(3)	1·374(3)
C61—C62	1·380(4)	1·395(4)	C61—C66	1·389(4)	1·405(2)
C62—C63	1·382(2)	1·387(2)	C63—C64	1·386(4)	1·333(2)
C64—C65	1·394(2)	1·355(4)	C65—C66	1·377(2)	1·400(2)
C411—C412	1·408(3)	1·394(3)	C411—C416	1·356(3)	1·373(3)
C412—C413	1·377(2)	1·386(2)	C413—C414	1·358(3)	1·370(3)
C414—C415	1·365(3)	1·359(3)	C415—C416	1·410(2)	1·411(2)
C421—C422	1·403(2)	1·393(4)	C421—C426	1·371(4)	1·399(2)
C422—C423	1·390(4)	1·389(4)	C423—C424	1·384(4)	1·392(2)
C424—C425	1·367(2)	1·348(4)	C425—C426	1·394(4)	1·376(4)

Atoms	Bond angle		Atoms	Bond angle	
C2—S1—C6	101·1(2)	101·6(2)	S1—C2—C21	112·9(3)	111·5(3)
S1—C2—C3	124·9(3)	124·9(2)	C2—C3—C4	127·8(3)	128·0(3)
C3—C4—C421	106·8(2)	106·6(2)	C3—C4—C411	110·6(2)	111·1(3)
C3—C4—C5	112·5(3)	111·1(3)	C5—C4—C421	108·8(2)	109·2(3)
C5—C4—C411	106·9(2)	106·9(2)	C4—C5—C6	127·7(3)	128·4(3)
S1—C6—C5	125·1(2)	125·1(3)	S1—C6—C61	113·5(3)	112·8(3)
C22—C21—C26	118·0(3)	117·3(3)	C21—C22—C23	122·0(3)	119·9(3)
C21—C26—C25	121·1(3)	121·7(3)	C62—C61—C66	118·4(3)	117·8(3)
C61—C62—C63	120·7(3)	119·8(3)	C61—C66—C65	121·8(3)	119·5(3)
C412—C411—C416	117·7(3)	118·0(3)	C411—C412—C413	120·6(3)	121·0(3)
C411—C416—C415	121·0(3)	120·7(3)	C422—C421—C426	117·7(3)	118·9(3)
C421—C422—C423	120·1(3)	120·3(3)	C421—C426—C425	122·0(3)	119·4(3)

TABLE IV

Selected conformational parameters of *I*, *II* and *III* with e.s.d.'s in parentheses. A, B symmetrically independent molecules in the unit cell

Parameter	*I*		*II*	*III*	
	A	B		A	B
Dihedral angles[a]					
P_1-P_2	4·6(2)	4·1(2)	4·3(1)	10·3(2)	1·3(2)
P_1-P_3	7·1(2)	6·6(3)	7·7(1)	14·7(3)	2·1(3)
P_1-Ph(2)	43·3(2)	41·6(1)	3·2(1)	49·1(1)	52·6(2)
P_1-Ph(6)	35·5(1)	36·0(1)	3·0(1)	30·1(2)	47·9(2)
P_1-Ph(41)	68·3(1)	67·8(1)	71·8(1)	71·1(1)	55·9(2)
P_1-Ph(42)	92·5(1)	91·9(1)	75·2(1)	81·7(1)	86·5(2)
Bond angles					
C3—C4—C411	110·6(2)	111·1(3)	111·3(2)	113·2(2)	112·1(2)
C3—C4—C421	106·8(2)	106·6(2)	107·3(2)	105·7(2)	108·5(2)
Torsion angles					
C3—C4—C411—C416	0·1(4)	1·2(4)	31·9(3)	24·6(4)	9·5(4)
C3—C4—C421—C426	69·6(4)	67·5(4)	63·7(2)	73·2(3)	66·5(3)
C411—C4—C421—C422	12·8(4)	13·0(4)	32·8(2)	49·5(4)	15·3(4)
C421—C4—C411—C412	62·6(4)	62·2(4)	58·3(2)	42·2(4)	70·2(4)

---

[a] P_1 means plane C2, C3, C5, C6; P_2 plane C2, X, C6; P_3 plane C3, C4, C5; Ph(*n*) mean plane of phenyl at the position *n*.

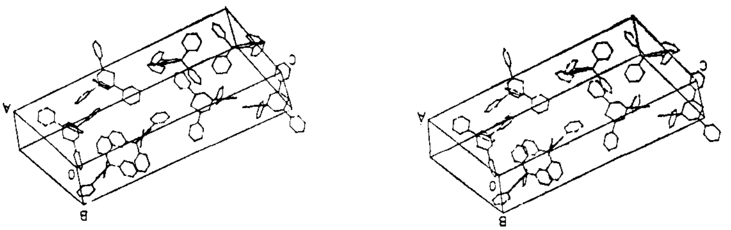

FIG. 2

Stereoscopic view of the unit cell of *I* (hydrogens omitted for clarity) observed no tendency to the parallel stacking of phenyl rings. There is no difference between the molecular geometry of independent molecules A and B beyond the range of 4 e.s.d.'s. The average bond lengths $\langle C(sp^2)—C(sp^3)\rangle$ = 1·52(1), $\langle C(sp^2)=C(\text{phenyl})\rangle$ = 1·49(1) and $\langle C(sp^3)—C(\text{phenyl})\rangle$ = 1·55(1) Å do not deviate from values observed with 1,4-dihydropyridines and 4*H*-pyrans[11,12,17]. The average double bond length $\langle C(sp^2)=C(sp^2)\rangle$ = 1·33(1) Å is shorter than the typical value[18]. This shortening has been observed and reported already in the previous studies of photochromic 1,4-dihydropyridines and 4*H*-pyrans[11,17]. The average bond length $\langle C(sp^2)—S\rangle$ = 1·75(1) Å. All phenyls deviate similarly from their ideal geometry, mainly due to the electron inductive effect[19] and the rigid body thermal motion[20]. The average inner phenyl angles are 118·0(5), 120·7(8), 120·5(9) and 119·6(6)° starting from the angle at the pivot atom. The torsion angles on the bonds connecting the phenyl to the C2 atom, i.e. C3—C2—C21—C26, are −41·1° and 40·3(2)° for A and B, respectively. The corresponding values for the phenyl at the site C6, i.e. C5—C6—C61—C62, are −38·2 and 38·8(1)°. The orientation of the phenyls at the site C4 is described by their orientation with respect to the plane of atoms C411, C4, C421. Torsion angles C411—C4—C421—C422 and C421—C4—C411—C412, are 12·8, 62·6° and 13·0(4), 62·2(4)° for A and B, respectively.

The molecular structure *I* is compared with two similar photochromic structures *II* and *III* in Table IV. For the sake of simplicity, the conformation of the central ring is described here using boat angles between the mean plane of double bonds P_1: $C(sp^2)$, $C(sp^2)$, $C(sp^2)$, $C(sp^2)$ and the planes P_2: $C(sp^2)$, X, $C(sp^2)$ and P_3: $C(sp^2)$, $C(sp^3)$, $C(sp^2)$, respectively. All structures show boat conformations of the central ring with the boat angles listed in Table IV. The deviations of $C(sp^2)$ atoms from the double bonds mean plane P_1 are less than 0·012 Å for all structures. The $C(sp^3)$ atom deviates from the plane P_1 more than the heteroatoms S and O, however less for N. With respect to our results obtained from the data of differently substituted 1,4-dihydropyridines[17] such a high deviation of N seems to be exceptional. The orientation of the mean planes Ph(2) and Ph(6) of phenyls at the positions 2 and 6 described simply by the dihedral angles between this plane and plane P_1 (see Table IV) is different in case of *II* than in the other ones. In spite of the very small rotation about 3·2 and 3·0(1)° for *II*, there is a significant rotation in the other cases. The deviations of the bonds C2—C21 and C6—C61 from the plane P_1 are less than 3° for all structures. As the equivalent orientation of the mean plane of phenyls at the position 4 relative to the mean plane P_1 is not illustrative enough, the torsion angles on C4—C421 and C4—C411 are listed in Table IV. By comparing the bond angles C3—C4—C411 and C3—C4—C421 we observed asymmetry in the position of these phenyl substituents reported and discussed before[21].

The absorption spectrum of diethyl ether solution of *I* is given in Fig. 3 (curve *1*). The maximum of absorption was found at the wavelength 240 nm. Polycrystalline material does not possess optical absorption for wavelengths longer than 370 nm

(Fig. 3, curve *2*). Immediately after the irradiation of *I* with light of λ_{exc} < c. 370 nm at room temperature violet colour appeared. The reflection spectrum (Fig. 3, curve *3*) showed that the main maximum of new absorption lies at 564 nm. It could be pointed out that absorption at c. 380 nm which appeared after the irradiation was mainly due to photodegradation. The long wave absorption photochromic process was found to be fully reversible, i.e. colouration by UV irradiation and thermal bleaching could be repeated many times. The cause of thermal bleaching is displayed in Fig. 4, curve *1*. This dependence could be linearized by plotting the logarithm of Munk-Kubelka's function $F(R_\infty) = K/S$ (where R_∞ is the diffuse reflectance of the sample, K is the absorption coefficient and S is the scattering coefficient) or the logarithm of the normalized reactant concentration $[M(t)]/[M(0)]$ versus t^α, α being 0·65 at room temperature (cf. Fig. 4, curve *2*.) Therefore, the bleaching reaction in a polycrystalline sample of *I* can be discussed in terms of dispersive kinetics. This model has often been applied to physical or chemical reactions occurring in irregular systems, even if the elementary step is a single energy level reaction[9,22,23]. Because of the short penetration length of excitation UV light and due to the high specific surface of our polycrystalline system (compound *I* mixed with MgO powder, 1 : 3), the greatest part of excitation takes place at the surface or in a layer close to the surface where the molecules are not embedded in a perfectly ordered crystalline matrix. Moreover, it can be assumed that each of the excited molecules interacts in a somewhat different way or to a somewhat different extent with neighbouring molecules. This might be the reason why simple first-order kinetics do not apply to the overall process.

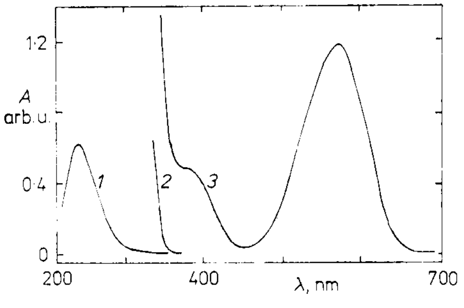

FIG. 3

Absorption spectra of *I* at room temperature: *1* spectrum in diethyl ether solution, *2* spectrum of polycrystalline powder mixed with MgO before UV excitation, *3* spectrum of the powder with MgO immediately after UV exposure

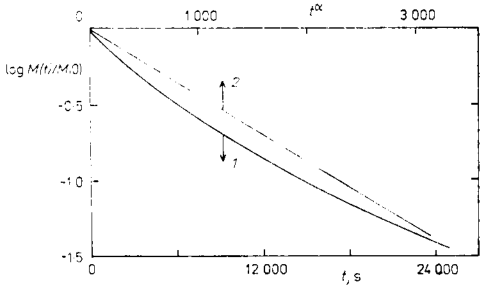

FIG. 4

Decay curves for thermal bleaching of *I* at 333 K in air: *1* a semilogarithmic plot of the normalized reactant concentration $[M(t)]/[M(0)]$ vs time t, *2* a semilogarithmic plot of $[M(t)]/[M(0)]$ vs t

It could be pointed out that the photochromic behaviour (i.e. both the spectra and kinetics courses) of *I*, is similar to compounds *II* and *III* (refs[8,9]). Thus, for *I* λ_{ph} = 537 nm, for *II* λ_{ph} = 586 nm and for *III* λ_{ph} = 568 nm. The thermal bleaching process can be described in terms of a dispersive first-order reaction in all cases.

This work was partially funded by Czechoslovak Academy of Sciences, grant No. 45028. We thank Mr P. Šebek for providing crystals and for valuable discussions.

REFERENCES

1. Machair R. N.: Photochem. Photobiol. *6*, 779 (1967).
2. Brown G. H.: *Photochromism.* Wiley, New York 1971.
3. Dürz H., Bonas-Larrent H.: *Photochromism.* Elsevier, Amsterdam 1990.
4. Peres de Cairalho A.: Ann. Chim. (Paris) *4*, 449 (1935).
5. Maeda K., Nakamura M., Sakai M.: J. Chem. Soc., Perkin Trans. 1 *1983*, 837.
6. Kurfürst A., Zeleny J., Schwartz M., Kuthan J.: Chem. Papers *41*, 623 (1987).
7. Shibuya J., Nabeshima M. (née Nakamura), Najamo H., Maeda K.: J. Chem. Soc., Perkin Trans. 2 *1988*, 1607.
8. Nešpůrek S., Schwartz M., Böhm S., Kuthan J.: Photochem. Photobiol., in press.
9. Nešpůrek S., Schnabel W.: Collect. Czech. Chem. Commun., in press.
10. Šebek P., Kuthan J., Böhm S., Nešpůrek S.: Photochem. Photobiol., in press.
11. Vojtěchovský J., Hašek J.: Acta Crystallogr., C *46*, 1727 (1990).
12. Iwasaki F., Maeda K., Watanabe T.: Bull. Chem. Soc. Jpn. *60*, 1255 (1987).
13. Debaerdemaeker T., Germain G., Main P., Tate C., Woolfson M. M.: *MULTAN 87. Computer Programs for the Automatic Solution of Crystal Structures from X-Ray Diffraction Data.* Universities of York, York 1987.
14. Sheldrick G. M.: *SHELX76. Program for Crystal Structure Refinement.* University of Cambridge, Cambridge 1976.
15. *International Tables for X-Ray Crystallography.* Vol. IV. Kynoch Press, Birmingham 1974.
16. Nardelli M.: *PARST. A System of Computer Koutines for Calculating Molecular Parameters. from Results of Crystal Structure Analysis.* University of Parma, Parma 1978.
17. Vojtěchovský J., Hašek J., Huml K., Ječný J.: Collect. Czech. Chem. Commun. *55*, 2059 (1990).
18. *International Tables for X-Ray Crystallography*, Vol. III. Kynoch Press, Birmingham 1962.
29. Domenicano A., Murray-Rust P., Vaciago A.: Acta Crystallogr., B *39*, 457 (1983).
20. Vojtěchovský J., Hašek J., Huml K., Schenk H., Goubitz K., De Ridder D., Fraanje J.: Acta Crystallogr., A *46*, C200 (1990).
21. Hašek J., Ondráček J.: Acta Crystallogr., C *46*, 1256 (1990).
22. Richert R., Bassler H.: Chem. Phys. Lett. *116*, 312 (1970).
23. Richert R.: Chem. Phys. Lett. *118*, 534 (1985).

Translated by L. Kopecká.